

Journal of
Mechanics of
Materials and Structures

**A NEW METHOD FOR CALCULATING THE PEAK TEMPERATURE
EVOLUTION IN THE ADIABATIC SHEAR BAND OF STEEL**

Xue-Bin Wang

Volume 5, N° 1

January 2010

 mathematical sciences publishers

A NEW METHOD FOR CALCULATING THE PEAK TEMPERATURE EVOLUTION IN THE ADIABATIC SHEAR BAND OF STEEL

XUE-BIN WANG

A new method for predicting the peak temperature evolution in the adiabatic shear band (ASB) of steel is proposed to overcome the drawback of the traditional method's underestimation of the peak temperature in the ASB. The average shear strain of a thin-walled tube in torsion is divided into three parts: the elastic shear strain, the average plastic shear strain outside the ASB, and the average plastic shear strain of the ASB. The relation between the shear stress acting on the tube and the average shear strain of the tube is established. The postpeak shear stress-average shear strain curve of the ASB is found to be dependent on the gage length. As an example, the shear stress-average plastic shear strain curve of the ASB is back-calculated from the measured shear stress-average shear strain curve of an AISI 1018 cold rolled steel tube. The peak temperature and average temperature in the ASB are calculated and compared with the experimental result. It is found that the calculated peak temperature is closer to or slightly higher than the experimental result. The latter is a satisfactory result due to the underestimated peak temperature in the ASB in experiments.

1. Introduction

At high strain rates, metals and alloys frequently show narrow bands of highly localised shear deformation, referred to as adiabatic shear bands (ASBs). ASBs can be generally observed in applications such as metal forming, perforation, impact on structures, ballistic impact, machining, torsion, explosive fragmentation, grinding, interfacial friction, powder compaction, and granular flow.

The localised shear deformation in ASBs is accompanied by a rapid temperature rise of a very short duration, softening the material and reducing its resistance to further plastic deformation. The accurate assessment of the peak temperature in ASBs is especially important in identifying whether the dynamic recovery, recrystallisation, or phase transformation occurs and in determining the extent of softening of the material and its load-carrying capacity. The temperature in ASBs is usually assessed by the plastic work determined by the area below the measured stress-strain curve of a specimen [Xu et al. 2001; 2008; Wei et al. 2004]. However, using the traditional method, only the average temperature in the specimen is assessed, rather than the peak temperature in the ASBs. Undoubtedly, the traditional method will underestimate the peak temperature in the ASBs.

Some researchers have measured the temperature distribution and evolution in ASBs using infrared detectors and infrared high-speed microscopic cameras. Hartley et al. [1987] observed ASBs in two kinds of steels and measured the temperature in the ASBs by determining the infrared radiation emitted at the metal surface. It was found that the maximum temperature rise in the ASBs was about 450°C and that the temperature distribution across the ASBs was consistent with results of stability analyses. A series of

Keywords: adiabatic shear band, steel, torsion, shear stress, shear strain.

experiments was performed by [Duffy and Chi \[1992\]](#) to study the process of ASB initiation and formation in steels. The local temperature in the ASB was measured by employing an array of small high-speed infrared detectors that provided a plot of temperature as a function of time and position. Within the ASB region, temperatures of 600°C were measured. Dynamic torsion experiments were conducted by [Cho et al. \[1993\]](#) and local temperature increases of up to 600°C were measured. [Zhou et al. \[1996\]](#) studied the initiation and propagation of ASBs by subjecting prenotched plates to asymmetric impact loading. The highest temperature measured was in excess of 1400°C. The results showed that the peak temperatures inside the propagating ASBs increased with impact velocity. [Liao and Duffy \[1998\]](#) investigated the process of initiation and formation of ASBs in Ti-6Al-4V. An array of infrared detectors was employed to measure the local temperature rise in ASBs during the deformation process. A peak temperature of 440–550°C was found in their tests. [Guduru et al. \[2001\]](#) investigated the initiation and propagation characteristics of ASBs in a type of steel. A developed two-dimensional high speed infrared camera was employed to observe the temperature field evolution during the initiation and propagation of ASBs. The results support the notion of a diffuse ASB tip and reveal “hot spots” distributed along the length of a well-developed ASB. ASBs in pure shear were studied in a type of steel and the temperature in the ASBs was obtained by [Giovanola \[1988\]](#). It was found that temperature elevation was in excess of 1000°C.

As is known, the thinness of ASBs (about ten to hundreds of microns) and the complex geometry of the thin-walled tube specimen render peak temperature measurement difficult. Actually, the highest temperatures measured in ASBs are usually lower than the phase transformation temperatures of steels or titanium alloys [[Xu et al. 2008](#)]. ASBs can be rapidly cooled by the surrounding bulk material in the deformational process. Besides this, the other reasons for the underestimated peak temperature in ASBs in experiments are:

- Only the temperature on the surface of a specimen is measured. Hence, the measured peak temperature perhaps will be underestimated since the material on the external surface of the specimen is readily cooled.
- In tests, the viewing area of one detector element can cover a portion of cooler adjacent material outside an ASB. Hence, the detector output undoubtedly underestimates the peak temperature in the ASB to some extent.

Recently, Wang introduced the gradient-dependent plasticity (GDP) where an internal length parameter was included in the yield function to describe the interactions and interplay among microstructures (the so-called microstructural effect) of heterogeneous metal materials [[De Borst and Mühlhaus 1992](#)] into the Johnson–Cook (J–C) and Zerilli–Armstrong (Z–A) models to investigate the temperature distribution and evolution in ASBs of Ti-6Al-4V and aluminium-lithium alloy [[Wang 2006a](#); [2006b](#); [2006c](#)], the strain and deformation distribution in ASBs of steels [[Wang 2007](#)], and the evolution of the transformed ASB thickness, local strain, and deformation at interfaces between the deformed and transformed ASBs [[Wang 2008](#)].

In the present paper, the J–C and Z–A models are abandoned and a new method for calculating the peak temperature evolution in the ASB is proposed. In the method, the measured shear stress–shear strain curve of a thin-walled tube in torsion is adopted. Using the measured curve, the shear stress–average plastic shear strain curve of the ASB can be back-calculated. Then, the peak temperature evolution in the ASB can be obtained. To this end, the relation between the shear stress acting on the tube and the average

shear strain of the tube must be established. The postpeak shear stress-average shear strain curve of the ASB is found to be dependent on the gage length. The predicted peak temperature evolution in the ASB is compared with the experimental result and the predicted value is closer to or slightly higher than the measured one. The latter is very reasonable since the peak temperature measured in tests is inevitably underestimated. The proposed method has a wide applicability for ductile metals and alloys.

2. Theoretical analysis

Derivation of the peak temperature in the ASB. The occurrence of ASBs is usually attributed to the thermal softening effect overcoming the strain-hardening effect. In this paper, for the sake of simplicity, an ASB is assumed to initiate just at peak shear stress τ_c (the maximum shear stress criterion).

Using three assumptions (the first is that the local plastic shear strain $\gamma_p(y)$ in the ASB is symmetrical with respect to the center of the ASB, the second is that the local plastic shear strain at the edges of the ASB is equal to the critical plastic shear strain, that is, the plastic shear strain corresponding to the maximum shear stress, and the third is that the actual thickness of the ASB corresponds to the maximum value of $\gamma_p(y)$), Wang has derived the expressions for $\gamma_p(y)$ and w (the thickness of the ASB) according to the GDP [Wang 2006a; 2006b; 2006c; 2007; 2008]:

$$\gamma_p(y) = \gamma_c + (\bar{\gamma}_p - \gamma_c) \cdot \left(1 + \cos \frac{y}{l}\right), \quad w = 2\pi l, \quad (1)$$

where l is the internal length parameter describing the heterogeneity of the material, $\bar{\gamma}_p$ is the average plastic shear strain of the ASB, γ_c is the critical plastic shear strain, y is the coordinate whose origin O is set at the center of the ASB (see Figure 1), and τ is the shear stress acting on the top and base of the ASB (see Figure 1).

The uniform temperature rise T_1 at prepeak is calculated as [Wang 2006a; 2006b; 2006c; 2007]

$$T_1 = \frac{\beta}{\rho C_p} \int_0^{\gamma_c} \tau d\bar{\gamma}_p, \quad (2)$$

where β is the work to heat conversion factor, C_p is the heat capacity, and ρ is the density.

Beyond the initiation of the ASB, the local plastic work $W_p(y)$ due to the microstructural effect done by the shear stress τ is [Wang 2006a; 2006b; 2006c; 2007]

$$W_p(y) = \int \tau d\gamma_p(y). \quad (3)$$

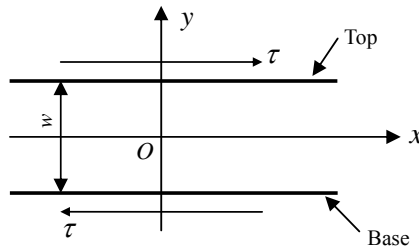


Figure 1. A narrow ASB in shear.

Using Equation (1)₁, (3) can be expressed as [Wang 2006a; 2006b; 2006c; 2007]

$$W_p(y) = \left(1 + \cos \frac{y}{l}\right) \int_{\gamma_c}^{\bar{\gamma}_p} \tau d\bar{\gamma}_p. \quad (4)$$

Thus, the local temperature distribution $T_m(y)$ in the ASB due to the microstructural effect is [Wang 2006a; 2006b; 2006c; 2007]

$$T_m(y) = \frac{\beta}{\rho C_p} \int \tau d\gamma_p(y) = \frac{\beta}{\rho C_p} \cdot \left(1 + \cos \frac{y}{l}\right) \int_{\gamma_c}^{\bar{\gamma}_p} \tau d\bar{\gamma}_p. \quad (5)$$

The peak temperature $T_m(0)$ in the ASB due to the microstructural effect is

$$T_m(0) = \frac{2\beta}{\rho C_p} \int_{\gamma_c}^{\bar{\gamma}_p} \tau d\bar{\gamma}_p. \quad (6)$$

The peak temperature $T(0)$ in the ASB is the sum of the initial temperature T_0 , the temperature rise T_1 at prepeak, and the peak temperature rise $T_m(0)$ at postpeak:

$$T(0) = T_0 + T_1 + T_m(0) = T_0 + \frac{\beta}{\rho C_p} \int_0^{\gamma_c} \tau d\bar{\gamma}_p + \frac{2\beta}{\rho C_p} \int_{\gamma_c}^{\bar{\gamma}_p} \tau d\bar{\gamma}_p. \quad (7)$$

The average temperature T_a in the ASB can be calculated as

$$T_a = T_0 + \frac{\beta}{\rho C_p} \int_0^{\bar{\gamma}_p} \tau d\bar{\gamma}_p. \quad (8)$$

Considering (8), (7) can be rewritten as

$$\begin{aligned} T(0) &= T_0 + \frac{\beta}{\rho C_p} \int_0^{\gamma_c} \tau d\bar{\gamma}_p + \frac{\beta}{\rho C_p} \int_{\gamma_c}^{\bar{\gamma}_p} \tau d\bar{\gamma}_p + \frac{\beta}{\rho C_p} \int_{\gamma_c}^{\bar{\gamma}_p} \tau d\bar{\gamma}_p \\ &= T_0 + \frac{\beta}{\rho C_p} \int_0^{\bar{\gamma}_p} \tau d\bar{\gamma}_p + \frac{\beta}{\rho C_p} \int_{\gamma_c}^{\bar{\gamma}_p} \tau d\bar{\gamma}_p = T_a + \frac{\beta}{\rho C_p} \int_{\gamma_c}^{\bar{\gamma}_p} \tau d\bar{\gamma}_p. \end{aligned} \quad (9)$$

Using (6), $T(0)$ is written as

$$T(0) = T_a + \frac{T_m(0)}{2}. \quad (10)$$

It is found from (9) and (10) that the peak temperature $T(0)$ in the ASB is always higher than the average value T_a beyond the occurrence of the ASB. The difference between the two kinds of temperatures is greater when the plastic work done by the shear stress is higher. Moreover, when β is higher, or ρ and C_p are lower, $T(0)$ will be greatly higher than T_a .

The peak temperature $T(0)$ in the ASB is dependent on the average temperature T_a and the shear stress-average plastic shear strain curve (τ - $\bar{\gamma}_p$ curve) of the ASB. This curve cannot be measured experimentally. Only the shear stress-average shear strain curve (τ - γ curve) of a specimen can be measured. When the tested specimen is subjected to localised failure in a form of an ASB beyond the peak shear stress, the size of the ASB will be smaller than the gage length of the specimen.

Derivation of the shear stress-average shear strain curve of a tube specimen. We will now establish the theoretical expression for the τ - γ curve of a tube specimen. Using this expression, the τ - $\bar{\gamma}_p$ curve of the ASB can be back-calculated from the measured τ - γ curve. Thus, the peak temperature $T(0)$ in the ASB can be assessed.

Figure 2 shows a thin-walled tube in torsion. We have drawn a straight line fg on the outer surface of the tube, which is parallel to the symmetric axis of the tube (see Figure 2a). In the elastically deformational stage and the strain-hardening stage, the deformation within the tube is considered to be uniform. Thus, the straight line fg will change to an inclined straight line $f'g$ (see Figure 2b). After an ASB is initiated at a position on the tube, the material outside the ASB will be unloaded elastically, while the material in the ASB will be subjected to a severe plastic shear deformation in the strain-softening process. Thus, the initial straight line fg will change to a complex pattern (see Figure 2c). In the ASB, $g'g''$ (also called a flow line) will be a curve. Outside the ASB, gg' and $f''g''$ are still two straight lines.

The size of the ASB is assumed to be w . Outside the ASB, the size of the uniformly deformational part is assumed to be L' . Thus, the gage length L of the tube is

$$L = L' + w. \quad (11)$$

The elastic shear strain γ^e within the tube is always seen as uniform. Thus, beyond the occurrence of the ASB, we have

$$\gamma^e = \frac{\tau}{G}, \quad (12)$$

where G is the shear elastic modulus.

The localised plastic shear deformation only exists in the ASB. Thus, the average value $\bar{\gamma}_a^p$ of the average plastic shear strain $\bar{\gamma}_p$ of the ASB over the entire tube is

$$\bar{\gamma}_a^p = \frac{\bar{\gamma}_p w}{L}. \quad (13)$$

The average value γ of the total shear strain of the tube will be composed of three parts beyond the occurrence of the ASB: the elastic shear strain γ^e , the average plastic shear strain $\gamma_c L'/L$ due to the uniformly plastic shear deformation outside the ASB, and the average plastic shear strain $\bar{\gamma}_a^p$ due to the

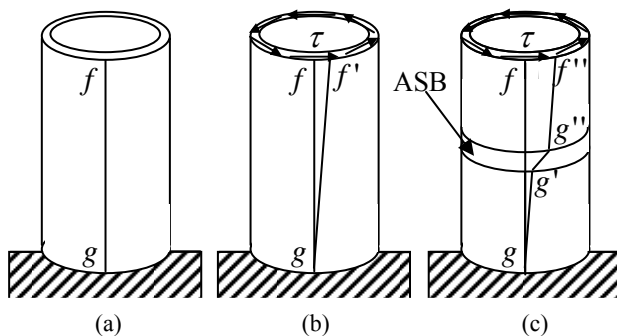


Figure 2. A thin-walled tube specimen without deformation (a), the uniform shear deformation in the elastic and strain-softening stages (b), and the localised shear deformation in the ASB and uniform shear deformation outside the ASB (c).

localised shear deformation in the ASB. Thus, we have

$$\gamma = \gamma_c \frac{L'}{L} + \gamma^e + \bar{\gamma}_a^p. \quad (14)$$

Using Equations (11)–(14), we have

$$\gamma = \frac{\gamma_c L'}{L' + w} + \frac{\tau}{G} + \frac{\bar{\gamma}_p^w}{L' + w}. \quad (15)$$

The shear stress-average shear strain curve (τ - γ curve) of a thin-walled tube can be measured in the torsional Kolsky bar experiment. It is found from (15) that after the ASB initiates, the measured postpeak τ - γ curve depends on the size of the gage length (L).

For a given thin-walled tube tested in torsion, one can determine the shear elastic modulus G and the critical plastic shear strain γ_c from the measured τ - γ curve. Once the thickness of the ASB is measured, the postpeak shear stress-average plastic shear strain curve (τ - $\bar{\gamma}_p$ curve) of the ASB can be back-calculated from the measured τ - γ curve. Thus, $T(0)$ can be calculated, see (9) and (10).

Calculation of the peak temperature in the ASB using the back-calculated shear stress-average plastic shear strain curve of the ASB. Herein, the back-calculated postpeak τ - $\bar{\gamma}_p$ curve of the ASB is approximated by n' linear segments (see Figure 3). When the shear stress τ decreases to τ_{i+1} from τ_i , the increment of the average plastic shear strain of the ASB is $\bar{\gamma}_p^{i+1} - \bar{\gamma}_p^i$. Therefore, (6) can be written as

$$T_m(0) = \frac{\beta}{\rho C_p} \sum_{i=1}^{n'} (\tau_i + \tau_{i+1}) \cdot (\bar{\gamma}_p^{i+1} - \bar{\gamma}_p^i). \quad (16)$$

Similarly, the prepeak τ - $\bar{\gamma}_p$ curve is approximated by m' linear segments. When the shear stress τ decreases or increases to τ_{j+1} from τ_j , the increment of the plastic shear strain is $\bar{\gamma}_p^{j+1} - \bar{\gamma}_p^j$. Therefore, Equation (2) can be written as

$$T_1 = \frac{\beta}{2\rho C_p} \sum_{j=1}^{m'} (\tau_j + \tau_{j+1}) \cdot (\bar{\gamma}_p^{j+1} - \bar{\gamma}_p^j). \quad (17)$$

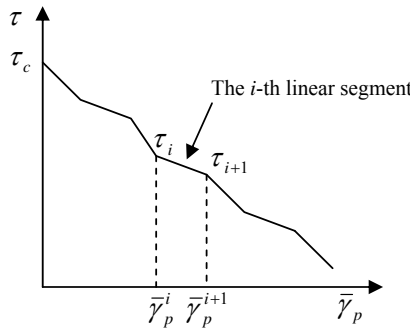


Figure 3. A schematic of the postpeak shear stress-average plastic shear strain relation of the ASB.

Thus, the peak temperature $T(0)$ in the ASB is

$$\begin{aligned}
 T(0) &= T_0 + T_1 + T_m(0) = T_0 + \frac{\beta}{2\rho C_p} \sum_{j=1}^{m'} (\tau_j + \tau_{j+1}) \cdot (\bar{\gamma}_p^{j+1} - \bar{\gamma}_p^j) + \frac{\beta}{\rho C_p} \sum_{i=1}^{n'} (\tau_i + \tau_{i+1}) \cdot (\bar{\gamma}_p^{i+1} - \bar{\gamma}_p^i) \\
 &= T_0 + \frac{\beta}{2\rho C_p} \sum_{j=1}^{m'} (\tau_j + \tau_{j+1}) \cdot (\bar{\gamma}_p^{j+1} - \bar{\gamma}_p^j) + \frac{\beta}{2\rho C_p} \sum_{i=1}^{n'} (\tau_i + \tau_{i+1}) \cdot (\bar{\gamma}_p^{i+1} - \bar{\gamma}_p^i) \\
 &\quad + \frac{\beta}{2\rho C_p} \sum_{i=1}^{n'} (\tau_i + \tau_{i+1}) \cdot (\bar{\gamma}_p^{i+1} - \bar{\gamma}_p^i) \\
 &= T_0 + \frac{\beta}{2\rho C_p} \sum_{k=1}^{n'+m'} (\tau_k + \tau_{k+1}) \cdot (\bar{\gamma}_p^{k+1} - \bar{\gamma}_p^k) + \frac{\beta}{2\rho C_p} \sum_{i=1}^{n'} (\tau_i + \tau_{i+1}) \cdot (\bar{\gamma}_p^{i+1} - \bar{\gamma}_p^i) \\
 &= T_a + \frac{\beta}{2\rho C_p} \sum_{i=1}^{n'} (\tau_i + \tau_{i+1}) \cdot (\bar{\gamma}_p^{i+1} - \bar{\gamma}_p^i). \tag{18}
 \end{aligned}$$

3. Examples and discussion

Calculation of the shear stress-average plastic shear strain curve of the ASB. For AISI 1018 cold rolled steel, [Hartley et al. \[1987\]](#) measured the shear stress-time curves of nine thin-walled tubes in torsion and the peak temperature evolution in ASBs. In their experiments, in order to determine the temperature profile within ASBs, each detector element was focused on a 20 micro spot size on the specimen. The maximum temperature rise recorded in their tests was about 420°C, significantly higher than the average temperature (240°C) measured with a 250 micro spot size.

The typical behaviour of shear stress and ASB peak temperature as functions of time are shown in [Figure 4](#), left, taken from [\[Hartley et al. 1987\]](#). In each experiment, the duration was 650 microseconds. The measured maximum average shear strain of the tube was 0.45. For the constant strain rate test, we can translate the shear stress-time curve into a τ - γ curve for the tube ([Figure 4](#), right).

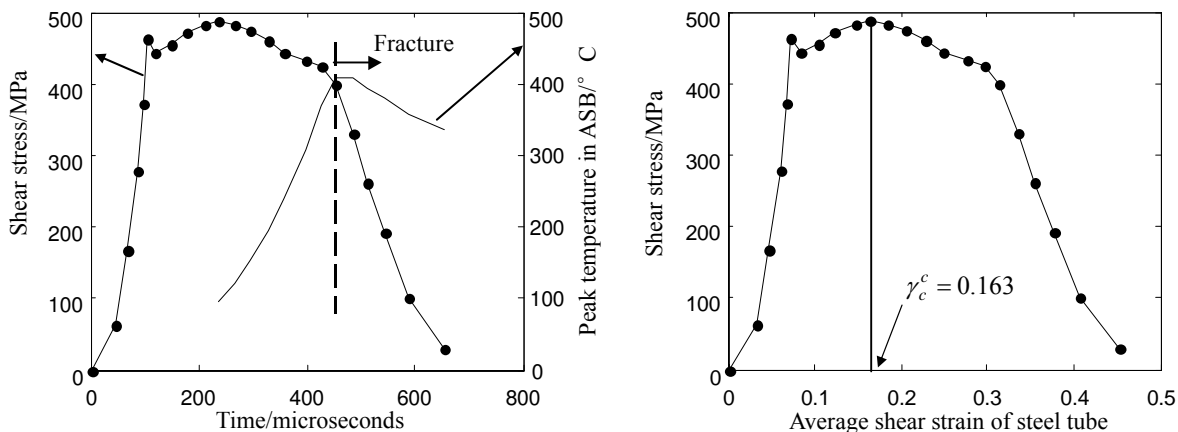


Figure 4. Left: Experimentally observed curves of shear stress and ASB peak temperature versus time. From [\[Hartley et al. 1987\]](#). Right: Shear stress versus average shear strain curve for a steel tube, based on values on the left.

It can be seen in [Figure 4](#) that the peak temperature in the ASB increases with decreasing shear stress beyond the peak shear stress. When fracture just occurs, the peak temperature reaches its maximum (about 680 K) and then drops slowly.

Prior to the peak stress, the elastic and plastic shear deformations within the tube can be considered to be uniform. After subtracting the elastic shear strain γ^e from the total shear strain γ , we can determine the prepeak $\tau-\bar{\gamma}_p$ curve. To back-calculate the $\tau-\bar{\gamma}_p$ curve of the ASB from the $\tau-\gamma$ curve, one needs to determine the values of G , L , w , and γ_c .

In the initial loading stage, the measured shear stress-time curve exhibits nonlinearity (see [Figure 4](#), right). The adopted value of the shear elastic modulus of AISI 1018 cold rolled steel is equal to the slope of the shear stress-shear strain curve in the linearly elastic stage, that is, $G = 10.328$ GPa.

The value of the gage length of the tube in the present calculation is assumed to be the gage length of the tube in the experiment (2.5 mm) of [Hartley et al. \[1987\]](#), that is, $L = 2.5$ mm.

The critical plastic shear strain γ_c is calculated as

$$\gamma_c = \gamma_c^c - \frac{\tau_c}{G}, \quad (19)$$

where γ_c^c is the shear strain corresponding to the peak shear stress τ_c . According to [Figure 4](#), right, γ_c^c and τ_c are 0.163 and 486 MPa, respectively. Thus, using [Equation \(19\)](#), we have $\gamma_c = 0.116$.

The reported thickness of the ASBs was about 0.3 mm [[Hartley et al. 1987](#)]. Considering the strain rate, plastic work, and thermal conductivity [[Dodd and Bai 1985](#)], the value calculated was 0.2 mm [[Dodd and Bai 1985](#); [Hartley et al. 1987](#)]. In this paper, the adopted values of the thickness of the ASB are 0.3 mm and 0.25 mm, respectively.

The calculated prepeak shear stress-plastic shear strain curve of the specimen and shear stress-average plastic shear strain curve of the ASB is shown in [Figure 5](#), left, with $G = 10.328$ GPa, $L = 2.5$ mm, $\gamma_c = 0.116$, and $w = 0.3$ mm. The calculated prepeak shear stress-plastic shear strain curve of the specimen and shear stress-average plastic shear strain curve of the ASB are shown in [Figure 5](#), right, with $G = 10.328$ GPa, $L = 2.5$ mm, $\gamma_c = 0.116$, and $w = 0.25$ mm. Five and seven linear segments are

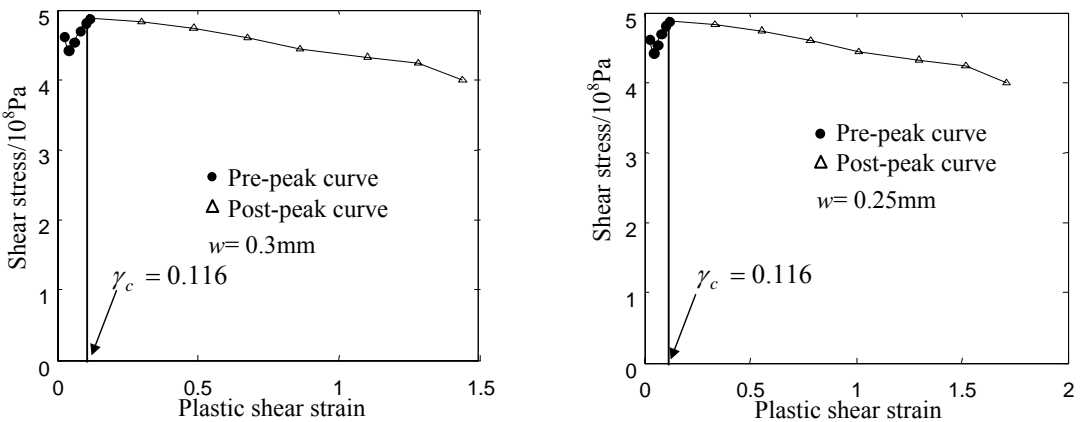


Figure 5. Calculated prepeak shear stress-plastic shear strain curve of the specimen and shear stress-average plastic shear strain curve of the ASB.

used to approximate the prepeak and postpeak parts of the $\tau-\bar{\gamma}_p$ curve, respectively, that is, $m' = 5$ and $n' = 7$.

In two graphs of Figure 5, the predicted maximum values of $\bar{\gamma}_p$ are 1.44 and 1.71, respectively. Therefore, the wider the ASB is, the lower the maximum value of the average plastic shear strain of the ASB is. In the left graph, the calculated maximum value of the average plastic shear strain of the ASB is about $1.44/0.116 = 12.4$ times the critical plastic shear strain corresponding to the initiation of the ASB. In the right graph, the maximum value is about $1.71/0.116 = 14.7$ times the initial value.

Comparison of the calculated peak and average temperatures in the ASB and the experimental result.

The top row of Figure 6 shows the evolution of $T(0)$ and T_a with decreasing shear stress, with parameters $w = 0.30$ mm,

$$C_p = 473 \text{ J/(kg}\cdot\text{K)}, \quad \rho = 7800 \text{ kg}\cdot\text{m}^{-3}, \quad T_0 + T_1 = 367 \text{ K}, \quad \beta = 0.95 \text{ (left) or } 0.85 \text{ (right)}. \quad (20)$$

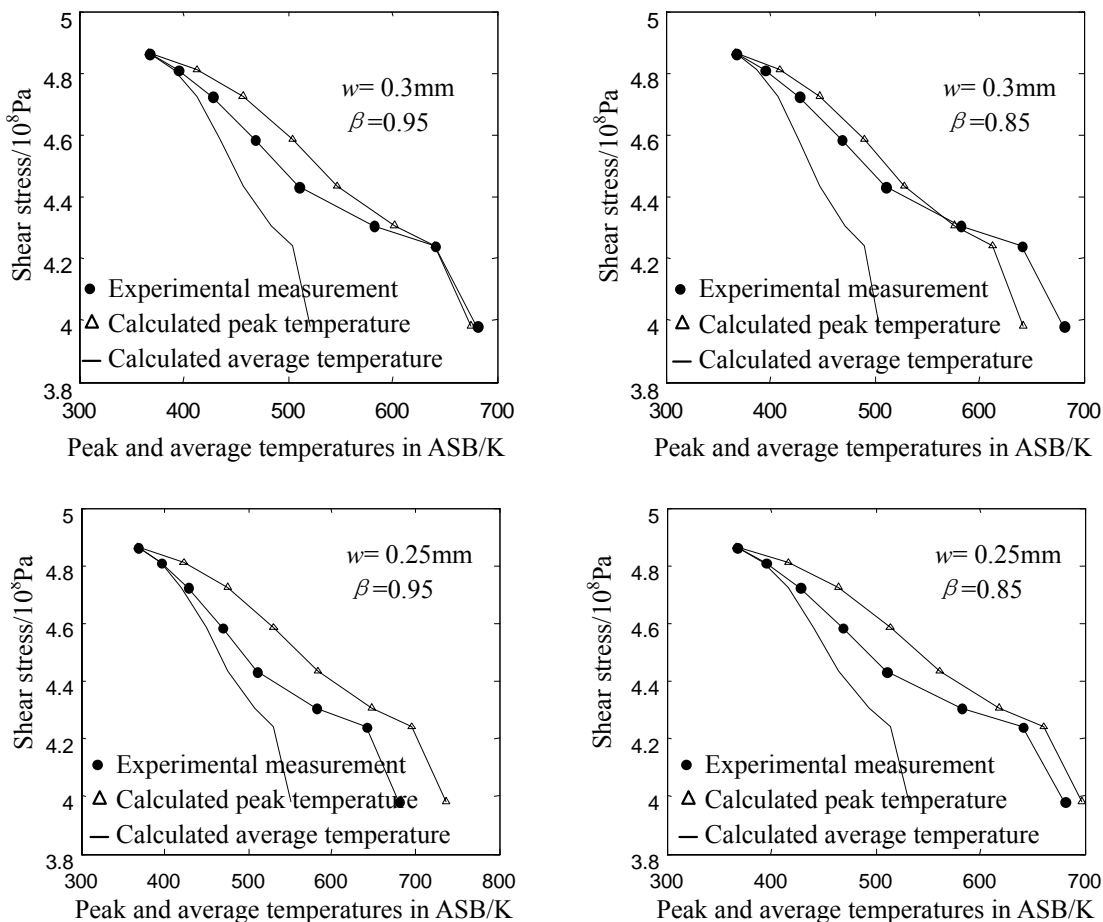


Figure 6. Predicted peak and average temperature evolution in the ASB with decreasing shear stress. For comparison we include experimental results from [Hartley et al. 1987].

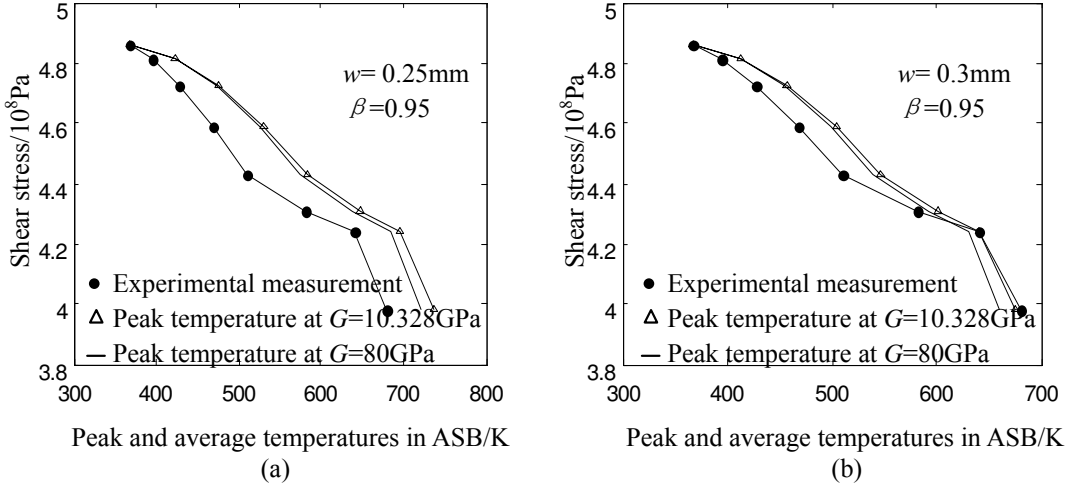


Figure 7. Effect of shear elastic modulus on the predicted peak temperature evolution in the ASB. For comparison we include experimental results from [Hartley et al. 1987].

together with the experimental measurements from [Hartley et al. 1987].

It is found from these graphs that both $T(0)$ and T_a increase with decreasing shear stress. The predicted value of $T(0)$ is even closer to the experimental result. The predicted maximum values of $T(0)$ are 675 K and 642 K, respectively, for the situations in these two graphs. The calculated peak temperature (675 K) in the ASB at $\beta = 0.95$ is slightly lower than the measured peak temperature in the ASB (680 K). When β decreases, $T(0)$ and T_a decrease.

The bottom row of Figure 6 shows the evolution of $T(0)$ and T_a with decreasing shear stress, $w = 0.25\text{ mm}$ and other parameters as in (20). Again we show the experimental measurements from [Hartley et al. 1987] for comparison.

It is found from these two graphs that the evolution of $T(0)$ with decreasing shear stress is still closer to the experimental result. The calculated value of the peak temperature in the ASB is always higher than the experimental measurement. The predicted maximum values of $T(0)$ are 737 K and 698 K, respectively, for the situations in these two graphs. The calculated peak temperature (698 K) in the ASB at $\beta = 0.85$ is slightly higher than the measured peak temperature in the ASB (680 K) — a very reasonable prediction given the underestimate of the peak temperature in the ASB in tests.

Effect of shear elastic modulus. As is known, the measured shear elastic modulus of any steel is about 80 GPa, while the value of the shear elastic modulus used in the situation depicted in Figures 5 and 6 is about 10 GPa, which is lower and is directly derived from the shear stress-average shear strain curve of a steel tube according to Figure 4. Herein, the shear elastic modulus of 80 GPa is used to calculate the peak temperature evolution in the ASB. In Figure 7, the calculated result with $G = 80\text{ GPa}$ is compared with the experimental results of [Hartley et al. 1987]; the other parameters are identical to those in 6, left column. The calculated results with $G = 10.328\text{ GPa}$ are also given in Figure 7. It is found that if the frequently cited shear elastic modulus of about 80 GPa is used, then the calculated peak temperatures are slightly lower than the results at $G = 10.328\text{ GPa}$. Moreover, the maximum temperature difference calculated

is only 17 K and 14 K, respectively, in the two parts of Figure 7. This suggests that the influence of the shear elastic modulus may be negligible.

4. Conclusions

The relation between the shear stress acting on a thin-walled tube in torsion and the average shear strain of the tube is established to back-calculate the shear stress-average plastic shear strain curve of the adiabatic shear band (ASB) from the shear stress-shear strain curve of the tube and then to calculate the peak temperature evolution in the ASB in the strain-softening process.

The peak and average temperatures in the ASB are calculated and compared with the experimental results of a AISI 1018 cold rolled steel tube. In a wider ASB, a lower maximum average plastic shear strain of the ASB is expected. A lower work to heat conversion factor leads to lower peak and average temperatures in the ASB. The maximum average plastic shear strain of the ASB is over ten times larger than the critical plastic shear strain corresponding to the initiation of the ASB.

The calculated peak temperature is very close to the experimental measurement. If the value (0.25 mm) of the ASB thickness used is slightly lower than the value (0.3 mm) reported by Hartley et al. [1987], then a reasonable prediction of the peak temperature in the ASB is obtained and the predicted value is slightly higher than the experimental result, which is reasonable since the ASB peak temperature is underestimated in experimental tests to some extent.

Acknowledgement. This research was supported by the Doctor Startup Foundation of Liaoning Province of China, No. 20081102. The author thanks Prof. Y. B. Xu, Institute of Metal Research, Chinese Academy of Sciences, for many useful discussions and encouragements.

References

- [Cho et al. 1993] K. M. Cho, S. Lee, S. R. Nutt, and J. Duffy, “Adiabatic shear band formation during dynamic torsional deformation of an HY-100 steel”, *Acta Metall. Mater.* **41** (1993), 923–932.
- [De Borst and Mühlhaus 1992] R. De Borst and H. B. Mühlhaus, “Gradient-dependent plasticity: formulation and algorithmic aspects”, *Int. J. Numer. Meth. Eng.* **35** (1992), 521–539.
- [Dodd and Bai 1985] B. Dodd and Y. Bai, “Width of adiabatic shear bands.”, *Mater. Sci. Tech.* **1** (1985), 38–40.
- [Duffy and Chi 1992] J. Duffy and Y. C. Chi, “On the measurement of local strain and temperature during the formation of adiabatic shear bands”, *Mater. Sci. Eng. A* **157** (1992), 195–210.
- [Giovanola 1988] J. H. Giovanola, “Adiabatic shear banding under pure shear loading, I: Direction observation of strain localization at energy dissipation measurement”, *Mech. Mater.* **7** (1988), 59–71.
- [Guduru et al. 2001] P. R. Guduru, A. J. Rosakis, and G. Ravichandran, “Dynamic shear bands: An investigation using high speed optical and infrared diagnostics”, *Mech. Mater.* **33** (2001), 371–402.
- [Hartley et al. 1987] K. A. Hartley, J. Duffy, and R. H. Hawley, “Measurement of the temperature profile during shear band formation in steels deforming at high strain rates”, *J. Mech. Phys. Solids* **35** (1987), 283–301.
- [Liao and Duffy 1998] S. C. Liao and J. Duffy, “Adiabatic shear bands in a Ti-6Al-4V Titanium alloy”, *J. Mech. Phys. Solids* **46** (1998), 2201–2231.
- [Wang 2006a] X. B. Wang, “Effects of constitutive parameters on adiabatic shear localization for ductile metal based on Johnson-Cook and gradient plasticity models”, *Trans. Nonferrous Met. Soc. China* **16** (2006a), 1362–1369.
- [Wang 2006b] X. B. Wang, “Temperature-dependent shear strain localization of aluminum-lithium alloy in uniaxial compression using Zerilli-Armstrong and gradient plasticity models”, *Mater. Sci. Forum* **519–521** (2006b), 789–794.

- [Wang 2006c] X. B. Wang, “Temperature distribution in adiabatic shear band for ductile metal based on Johnson-Cook and gradient plasticity models”, *Trans. Nonferrous Met. Soc. China* **16** (2006c), 333–338.
- [Wang 2007] X. B. Wang, “Adiabatic shear localization for steels based on Johnson-Cook model and second- and fourth-order gradient plasticity models”, *J. Iron Steel Res., Int.* **14** (2007), 56–61.
- [Wang 2008] X. B. Wang, “Effects of temperature and strain rate on the evolution of thickness of transformed adiabatic shear band”, *Solid State Phenom.* **138** (2008), 385–392.
- [Wei et al. 2004] Q. Wei, L. Kecskes, T. Jiao, K. T. Hartwig, K. T. R. , and E. Ma, “Adiabatic shear banding in ultrafine-grained Fe processed by severe plastic deformation”, *Acta Mater.* **52** (2004), 1859–1869.
- [Xu et al. 2001] Y. B. Xu, W. L. Zhong, Y. J. Chen, L. T. Shen, Q. Liu, Y. L. Bai, and M. A. Meyers, “Shear localization and recrystallization in dynamic deformation of 8090 Al-Li alloy”, *Mater. Sci. Eng. A* **299** (2001), 287–295.
- [Xu et al. 2008] Y. B. Xu, J. H. Zhang, Y. L. Bai, and M. A. Meyers, “Shear localization in dynamic deformation: Microstructural evolution”, *Metall. Mater. Trans. A* **39** (2008), 811–843.
- [Zhou et al. 1996] M. Zhou, A. J. Rosakis, and G. Ravichandran, “Dynamically propagating shear bands in impact-loaded prenotched plates, I: Experimental investigations of temperature signatures and propagation speed”, *J. Mech. Phys. Solids* **44** (1996), 981–1006.

Received 13 Mar 2009. Revised 20 Jul 2009. Accepted 30 Jul 2009.

XUE-BIN WANG: wxbbb@263.net

Department of Mechanics and Engineering Sciences, Liaoning Technical University, Fuxin 123000, China